The Astrophysical Journal, 776:116 (6pp), 2013 October 20 doi:10.1088/0004-637X/776/2/116

X-RAY SCALING RELATION IN EARLY-TYPE GALAXIES: DARK MATTER AS A PRIMARY FACTOR IN RETAINING HOT GAS

Dong-Woo Kim and Giuseppina Fabbiano
Smithsonian Astrophysical Observatory, 60 Garden Street, Cambridge, MA 02138, USA
Received 2013 April 23; accepted 2013 August 26; published 2013 October 7

ABSTRACT

We have revisited the X-ray scaling relations of early-type galaxies (ETG) by investigating, for the first time, the $L_{X,Gas}$–M_{Total} relation in a sample of 14 ETGs. In contrast to the large scatter (a factor of 10^2–10^3) in the $L_{X,Total}$–L_B relation, we found a tight correlation between these physically motivated quantities with an rms deviation of a factor of three in $L_{X,Gas} = 10^{38}$–10^{43} erg s^{-1} or M_{Total} = a few $\times$ 10^{10} to a few $\times$ 10^{12} $M_\odot$. More striking, this relation becomes even tighter with an rms deviation of a factor of 1.3 among the gas-rich galaxies (with $L_{X,Gas} > 10^{40}$ erg s^{-1}). In a simple power-law form, the new relation is $(L_{X,Gas}/10^{40}$ erg s$^{-1}) = (M_{Total}/3.2 \times 10^{11}\, M_\odot)^3$. This relation is also consistent with the steep relation between the gas luminosity and temperature, $L_{X,Gas} \sim T_{Gas}{}^{4.5}$, identified by Boroson et al., if the gas is virialized. Our results indicate that the total mass of an ETG is the primary factor in regulating the amount of hot gas. Among the gas-poor galaxies (with $L_{X,Gas}$ < a few $\times$ 10^{39} erg s^{-1}), the scatter in the $L_{X,Gas}$–M_{Total} (and $L_{X,Gas}$–T_{Gas}) relation increases, suggesting that secondary factors (e.g., rotation, flattening, star formation history, cold gas, environment, etc.) may become important.

Key words: galaxies: elliptical and lenticular, cD – X-rays: galaxies

Online-only material: color figure

1. INTRODUCTION

The "L_X–L_B" relation (or L_X–$L_{Optical}$, L_X–L_K; we will use L_X–L_K in this paper) of early-type galaxies (ETG; i.e., E and S0,) has been widely discussed since its first formulation by Trinchieri & Fabbiano (1985) and Forman et al. (1985). This relation, linking the stellar mass of ETGs with their total (∼0.5–5 keV) X-ray luminosity, which is an approximated proxy for the amount of hot gas they can retain, has been related to the gravitational confinement of the hot gas, and has been used to investigate the origin and evolution of the hot interstellar medium (ISM) of ETGs, including the effects of interactions in galaxy clusters and winds from stellar and active galactic nucleus (AGN) feedback (e.g., see review in Fabbiano 1989 and Mathews & Brighenti 2003; also Canizares et al. 1987; Ciotti et al. 1991; David et al. 1991; White & Sarazin 1991). The structural parameters of the ETG also appear to be relevant for the hot gas retention. "Boxy" galaxies with a central core tend to have larger amounts of hot gas than "disky" galaxies with central stellar cusps and fast rotation (Bender et al. 1989; Eskridge et al. 1995b; Pellegrini 2005). Core ETGs also tend to be larger and have older stellar populations, leading Kormendy et al. (2009) to suggest that the hot ISM may provide the working surface necessary for feedback by storing and smoothing episodic energy input and by shielding against the accretion of fresh gas, and thus impeding star formation (see also Binney 2004; Nipoti & Binney 2007).

The main characteristic of the L_X–L_K relation, which all of the above studies have tried to explain, is its large spread. For a given ETG optical luminosity L_K (i.e., stellar mass), L_X can vary by a factor of ∼100 in different ETGs (e.g., Fabbiano 1989; Eskridge et al. 1995a; Ellis & O'Sullivan 2006). However, the real spread is even larger because the X-ray luminosity L_X used in most published studies, as a proxy of the hot gas content, is the total integrated L_X of an ETG galaxy, which contains a significant contribution from the integrated input of stellar sources, including low-mass X-ray binaries (LMXBs; as first pointed out by Trinchieri & Fabbiano 1985). With the sub-arcsecond resolution of the *Chandra X-ray Observatory*, we are now able to measure the hot gas luminosity, $L_{X,Gas}$, by excluding individually detected LMXBs (see the review by Fabbiano 2006) and nuclear sources. We can also estimate and subtract the contribution of undetected stellar sources (faint LMXBs, active binaries, and cataclysmic variables) by fitting the X-ray spectra with multiple components (Boroson et al. 2011, hereafter BKF) and extrapolating to low luminosities the X-ray luminosity function of LMXBs (e.g., Figure 4 in Kim & Fabbiano 2010). The accurate subtraction of these contaminants is most critical in gas-poor galaxies, where the X-ray luminosity of the hot gas can be commensurable with or lower than that of the stellar sources. When the data are cleaned, we obtain a range of scatter in $L_{X,Gas}/L_K$ that can be as large as a factor of ∼10^3 or more (BKF).

This noisy scaling relation suggests that we may be trying to correlate the wrong quantities. The optical luminosity (L_K) is a good proxy for the integrated stellar mass of the galaxy, $M_\star$; however, it does not measure the amount of dark matter (DM) mass, which may be prevalent, especially at large radii. The total mass (stellar + DM), out to radii comparable to the total extent of the hot halos of gas-rich ETGs, is the physical quantity we must know in order to explore the importance of gravitational confinement for the hot gas retention (see Mathews et al. 2006). The amount of gas mass itself is small in ETGs and not important for gravitational confinement (e.g., Canizares et al. 1987). While dynamical masses have been measured using integral field two-dimensional spectroscopic data for a large number of ETGs (e.g., in the Atlas 3D sample; Cappellari et al. 2013), these data are limited to radii within $r < 0.5$–$1\, R_e$ (effective radius or half light radius), smaller than the extent of the hot gas in gas-rich ETGs, and so are not optimal for our purpose. However, a number of dynamical mass measurements at large radii have recently become available from the analysis of the kinematics of hundreds of globular clusters (GC) and planetary nebulae (PN) in individual galaxies (Deason et al. 2012).

Given these improvements in both X-ray and mass measurements, we have revisited the scaling relations of ETGs by

Table 1
Galaxy Sample

Name	T	d (Mpc)	log L_K ($L_\odot$)	M ($<5\,R_e$) (10^{11} $M_\odot$)	$L_{X,Gas}$ (10^{40} erg s^{-1})	Reference
(1)	(2)	(3)	(4)	(5)	(6)	(7)
N0821	−5	24.10	10.93	2.7 (0.6)	0.025 (−0.020 +0.022)	This work
N1399	−5	19.95	11.40	12.8 (1.8)	49.2 (−1.28 +1.28)	O'Sullivan
N1407	−5	28.84	11.57	11.0 (1.5)	15.9 (−1.86 +1.86)	O'Sullivan
N3377	−5	11.22	10.45	0.7 (0.2)	0.010 (−0.006 +0.007)	This work
N3379	−5	10.57	10.87	1.4 (0.2)	0.042 (−0.016 +0.016)	This work
N4374	−5	18.37	11.37	16.5 (2.0)	6.65 (−1.18 +1.18)	O'Sullivan
N4486	−4	16.07	11.41	30.6 (3.1)	905.5 (−1.32 +1.32)	O'Sullivan
N4494	−5	17.06	10.99	1.2 (0.2)	0.097 (−0.077 +0.078)	This work
N4564	−5	15.00	10.50	0.4 (0.1)	0.038 (−0.019 +0.020)	This work
N4636	−5	14.66	11.09	10.7 (1.9)	31.7 (−0.62 +0.62)	O'Sullivan
N4649	−5	16.83	11.48	8.7 (1.3)	18.3 (−1.54 +1.54)	O'Sullivan
N4697	−5	11.75	10.92	1.5 (0.2)	0.184 (−0.019 +0.038)	This work
N5128	−2	4.21	11.00	4.9 (0.5)	1.93 (−0.14 +0.14)	Kraft
N5846	−5	24.89	11.34	11.7 (2.8)	50.5 (−1.10 +1.10)	O'Sullivan

Notes.
(1) Galaxy name; (2) morphological type from RC3; (3) distance from Tonry et al. (2001); (4) K-band luminosity from 2MASS (assuming $K_\odot = 3.33$ mag); (5) total mass within five effective radii taken from Deason et al. (2012) after correcting for slightly different distances; (6) X-ray luminosity in 0.3–8 keV from the hot gas (see reference), with the error as explained in the text; (7) references for $L_{X,Gas}$: O'Sullivan et al. (2001); Kraft et al. (2003); this work (see Table 2).

investigating, for the first time, the $L_{X,Gas}$–M_{Total} relation in a sample of 14 ETGs, for which both X-ray and kinematics data are available. The results are presented in this paper. In Section 2, we describe our sample selection, *Chandra* observations, and data reduction techniques. In Section 3, we present the X-ray scaling relations of ETGs. In Section 4, we discuss the implications of our results.

2. GALAXY SAMPLE AND X-RAY DATA ANALYSIS

For the total mass of galaxies, we use the direct mass measurements from optical kinematics data of GCs from the SLUGGS survey and PNs from the PN.S survey. Deason et al. (2012) compiled optical data for 15 ETGs from the literature and provided a homogeneous data set of masses within $5\,R_e$. Fourteen of them were observed by *Chandra* for longer than 15 ks and are used in this study (see Table 1). NGC 1344 is not used here because its exposure is too shallow (3 ks) to measure the necessary gas properties.

For six gas-poor galaxies, we measure $L_{X,Gas}$ with the archived *Chandra* ACIS data (see Table 2). All galaxies were observed on the back-illuminated S3 chip, which has the better response at the energy range of interest (<2 keV) than the front-illuminated chip. As the entire gas emission is typically confined within a single CCD chip, we only analyze the data on the S3 chip. In hot gas-poor galaxies, the X-ray luminosity of hot gas, $L_{X,Gas}$, is often lower than that of LMXBs and in extremely gas-poor galaxies, $L_{X,Gas}$ is even lower than that of active binaries (AB) and cataclysmic variables (CV), $L_{X,AB+CV}$, which is about one-tenth of $L_{X,LMXB}$ (see BKF). Therefore, to accurately determine $L_{X,Gas}$ it is critical to properly subtract all stellar contributions. Following the technique of BKF, we separate the stellar and AGN contribution from the gaseous emission. Most bright LMXBs are detected in *Chandra* observations and excluded. We then fit the remaining diffuse emission in 0.3–5 keV with a four-component model, which consists of thermal plasma APEC for hot gas + 7 keV thermal Bremsstrahlung for undetected LMXBs + additional two components (APEC + power-law) for a population of ABs+CVs. In all cases, the hard component for undetected LMXBs is consistent within the error with those expected by extrapolating the X-ray luminosity function of LMXBs (Kim & Fabbiano 2010; see also Section 3.4.2 in BKF). For ABs and CVs, we use the spectral parameters determined with the *Chandra* spectra of M31 and M32 where all LMXBs can be detected and removed (see the Appendix in BKF). The normalizations are scaled based on the K-band luminosity within the region of interest. Although the error of the AB+CV component is not reflected in the statistical error of $L_{X,Gas}$, its contribution to the error of $L_{X,Gas}$ is small. For extremely gas-poor galaxies where $L_{X,Gas}$ is lower than that of the soft (APEC) component of AB+CV, we consider the error of the soft component of the AB+CV components (taken from BKF) and add the corresponding error in quadrature to the statistical error. The error of the hard component (power-law) of AB+CV may affect $L_{X,LMXB}$, but its effect is negligible. We note that our measurements are somewhat improved over those of BKF by applying Cash statistics for low signal-to-noise data and/or by grouping with a large number of counts, particularly when a large portion of hot gas emission is embedded with brighter point sources (e.g., in NGC 821).

For the remaining well-studied gas-rich galaxies, we adopt $L_{X,Gas}$ from the literature. For NGC 5128 (Cen A), which is rather complex with jets and various features, we take $L_{X,Gas}$ (corrected for a different distance and energy band) from Kraft et al. (2003), who analyzed *Chandra* ACIS-I and *XMM-Newton* data. For seven gas-rich Es, we take $L_{X,Total}$ from the *ROSAT* measurements by O'Sullivan et al. (2001). We correct it for the different distance and subtract $L_{X,LMXB}$ by applying the scaling relation between $L_{X,LMXB}$ and L_K from BKF ($L_{X,LMXB}/L_K = 10^{29}$ erg s^{-1} $L_{K\odot}{}^{-1}$). Because of the scatter in this relation, $L_{X,LMXB}$ may vary by ∼50% (BKF). For N4374 (M84), which has the lowest L_X among these seven galaxies, this scatter could cause an error of 18% in $L_{X,Gas}$. For the other gas-rich galaxies, this error is less than 10%. We added this error in Table 1.

Although derived physical quantities (such as spectral parameters and their spatial variations) are best measured with the

Table 2
Hot Gas Properties Measured in This Work

Name	ObsID	Exp. (ks)	R ($''$)	T (keV)	$L_{X,Total}$ (10^{40} erg s^{-1})	$L_{X,Gas}$ (10^{40} erg s^{-1})
(1)	(2)	(3)	(4)	(5)	(6)	(7)
N0821	a	209	30	0.09 (. . . . .)	0.883	0.025 (−0.020 +0.022)
N3377	02934	39	30	0.19 (. . . +0.07)	0.306	0.010 (−0.006 +0.007)
N3379	b	324	90	0.25 (−0.02 +0.02)	0.864	0.042 (−0.016 +0.016)
N4494	02079	15	30	0.62 (−0.34 +0.22)	1.440	0.097 (−0.077 +0.078)
N4564	04008	17	30	0.27 (. . . +0.45)	0.285	0.038 (−0.019 +0.020)
N4697	c	132	60	0.31 (−0.00 +0.01)	1.252	0.184 (−0.019 +0.038)

Notes.
(1) Galaxy name; (2) *Chandra* observation IDs: (a) 04006, 04408, 05691, 05692, 06310, 06313, 06314; (b) 01587, 07073, 07074, 07075, 07076; (c) 04727, 04728, 04729, 04730; (3) total *Chandra* exposure time in ks, after excluding background flares; (4) radius within which the hot gas emission is extracted; (5) temperature of hot gas; (6) total X-ray luminosity in 0.3–8 keV; (7) X-ray luminosity from the hot gas in 0.3–8 keV.

more sensitive *Chandra* data, the total gas luminosity measured by *ROSAT* data is still robust for most gas-rich galaxies, where some emission from the outskirt may be missed with *Chandra*'s smaller field of view. Because of the limited field of view of the *Chandra* ACIS chip, the extended gas emission ($r > 4'$) of gas-rich galaxies falls beyond the main ACIS back-illuminated S3 chip and a part of emission also falls in the gaps between S3 and S2 chips (because a target is usually located on axis, which is $\sim 2'$ off from the center of S3 toward S2). Taking this limitation in mind, we remeasure $L_{X,Gas}$ of three gas-rich galaxies (NGC 1407, NGC 4374, and NGC 5846) with the smallest angular extents (but still more extended than the S3 field of view) by analyzing S3 and S2 data and confirm that there is no systematic bias caused by using the *ROSAT* measurements. Our measurements of $L_{X,Gas}$ are about 10%–20% lower than those in Table 1, as expected by the "missed" emission. For M87, the AGN and jets may not be fully separated in the *ROSAT* data, but their contributions are only 0.6% (Pellegrini 2010) and 2% (Harris & Krawczynski 2006), respectively, and therefore have no effect on our results.

3. THE $L_{X,Gas}$ –M_{Total} RELATION

We show in Figure 1 the $L_{X,Gas}$–L_K relation for our 14 ETGs. Although the sample is small, Figure 1 clearly shows that the $L_{X,Gas}$–M_{Total} relation is tight. The best-fit relation in the form of $L_{X,Gas} \sim M_{Total}{}^{\alpha}$ has a slope of $\alpha = 2.7 \pm 0.3$ (dashed line in Figure 1). The rms deviation from this best fit is 0.5 dex (or a factor of three), which is considerably lower than the factor of $\sim 10^2$ scatter often seen in previous relations between $L_{X,Total}$ and L_B (e.g., Fabbiano 1989; Eskridge et al. 1995a; Ellis & O'Sullivan 2006) and the factor of $\sim 10^3$ scatter in the $L_{X,Gas}$–L_K relation (BKF; see below, Figure 2). Even more striking, this relation is extremely tight among the gas-rich ETGs with $L_{X,Gas} > 10^{40}$ erg s^{-1}. The only exception is M84 (NGC 4374). Because M84 is known to suffer from ongoing ram pressure stripping (e.g., Randall et al. 2008), the lower $L_{X,Gas}$ (an order of magnitude below those of other galaxies with similar M_{Total}) can be understood. The solid diagonal line indicates the best-fit relation among gas-rich ETGs (excluding M84) with a slope of $\alpha = 3.3 \pm 0.3$. The rms deviation from this best fit is reduced to only 0.128 dex (or a factor of 1.3). This is the tightest relation ever reported in any relation involving the X-ray luminosity of ETGs. If we simplify the relation by fixing $\alpha = 3$ (see Section 4 for its justification), the best-fit relation is

$$(L_{X,Gas}/10^{40}\,\mathrm{erg\,s^{-1}}) = (M_{Total}/3.2 \times 10^{11}\,M_{\odot})^3.$$

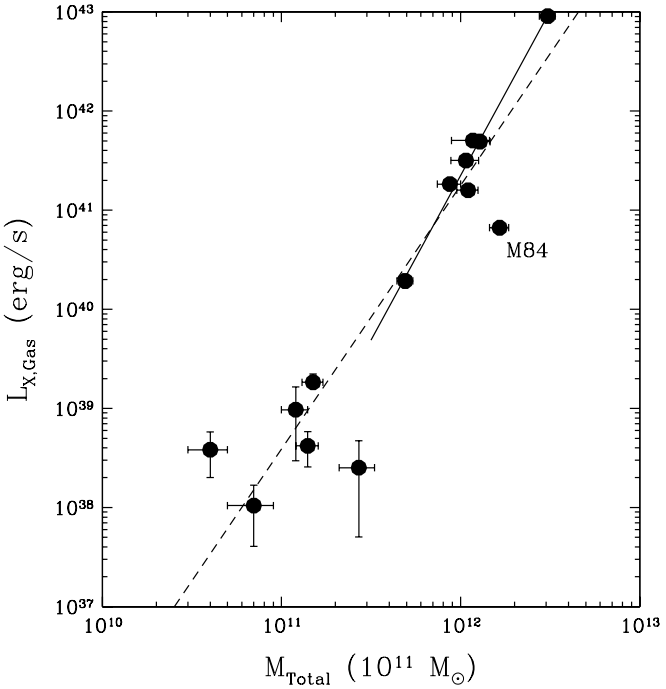

Figure 1. X-ray luminosities from the hot gas are plotted against M_{Total} ($<5\ R_e$) taken from Deason et al. (2012). The dashed line indicates the best fit using the entire sample ($L_{X,Gas} \sim M_{total}{}^{2.7}$) and the solid line is for gas-rich ETGs with $L_{X,Gas} > 10^{40}$ erg s^{-1} ($L_{X,Gas} \sim M_{total}{}^{3.3}$).

M87 is highest in both $L_{X,Gas}$ and M_{Total}; therefore, this single galaxy may have a strong leverage in dictating the relation. Moreover, because M87 is in the center of the Virgo cluster, its parameters may reflect an entire cluster rather than a single galaxy (although it was already noted with *Einstein* data that the gas in M87 is cooler, less luminous, and less extended than more regular clusters; e.g., Section 5.8 in Sarazin 1988). However, if we exclude M87, the relation remains identical, although with a slightly larger error ($\alpha = 3.3 \pm 0.5$) and a slightly larger rms deviation (0.138 dex or a factor of 1.4).

For comparison, we also plot the $L_{X,Gas}$–L_K relation in Figure 2. In addition to the 14 ETGs of Figure 1, we show other normal ETGs from the BKF sample (smaller, open symbols)

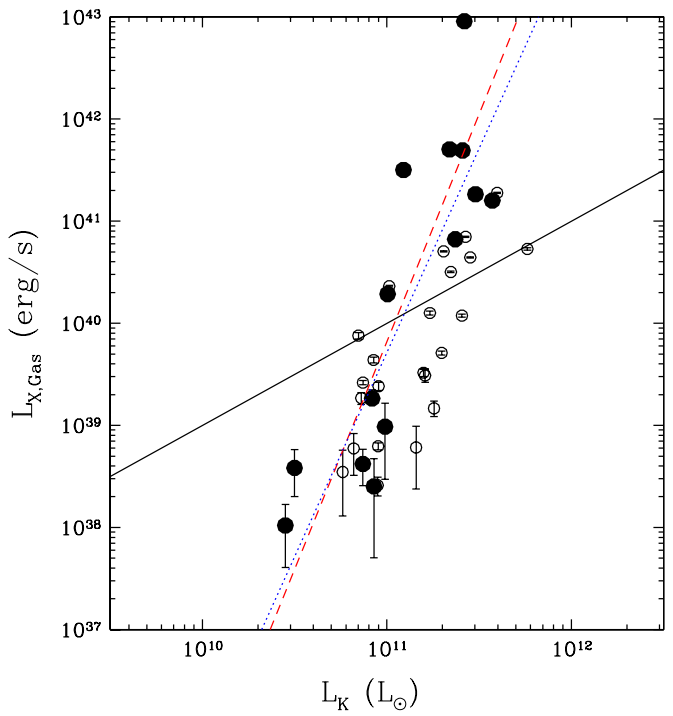

Figure 2. X-ray luminosities from the hot gas are plotted against L_K. The small open circles are additional galaxies from the BKF sample. The solid line indicates L_X expected from LMXBs. The (red) dashed and (blue) dotted lines indicate the best fit relations with ($L_{X,Gas} \sim {L_K}^{4.5}$) and without M87 ($L_{X,Gas} \sim {L_K}^4$).

(A color version of this figure is available in the online journal.)

which nicely fill the parameter space with intermediate $L_{X,Gas}$. The $L_{X,Gas}$–L_K relation is very steep, $L_{X,Gas} \sim {L_K}^{4.5\pm0.8}$. If M87 is excluded, the relation becomes slightly flatter ($L_{X,Gas} \sim {L_K}^{4.0\pm0.7}$), but statistically the slope remains the same. This relation can be compared with the widely used $L_{X,Total}$–L_B relation (e.g., see Figure 48 in Kormendy et al. 2009), but becomes steeper because of the considerably lower $L_{X,Gas}$ compared to the $L_{X,Total}$ in gas-poor galaxies. The solid diagonal line in Figure 2 indicates the expected X-ray luminosity from the population of LMXBs (using the linear relation of $L_{X,LMXB}/L_K = 10^{29}$ erg s^{-1} ${L_{K\odot}}^{-1}$ taken from BKF). For a large number of ETGs, the hot gas luminosity is lower than the integrated contribution of LMXBs. In extreme cases, the gas luminosity is even lower than that of ABs and CVs, which is about an order of magnitude lower than that of LMXBs (BKF). We note that our $L_{X,Gas}$–L_K relation is steeper than any previous relation of $L_{X,Total}$–L_K and also $L_{X,Gas}$–L_K, if the latter did not fully consider the contribution from ABs and CVs. Consequently, the $L_{X,Gas}$–L_K relation is much steeper than the $L_{X,Gas}$–M_{Total} relation and with a considerably larger scatter. The very tight $L_{X,Gas}$–M_{Total} relation seen among the gas-rich ETGs with $L_{X,Gas} > 10^{40}$ erg s^{-1} disappears in the $L_{X,Gas}$–L_K relation. Instead, a large range in $L_{X,Gas}$ (a factor of $\sim 10^3$) is clearly visible among galaxies with similar $L_K = 1$–2×10^{11} $L_{K\odot}$.

4. DISCUSSION

As discussed above (Section 1), the large scatter in L_X/L_B (a factor of 10^2) has been one of the long-standing puzzles in the field of extragalactic X-ray astronomy, ever since the *Einstein Observatory* provided the first X-ray images of ETG galaxies (see the review by Fabbiano 1989). Now, due to the *Chandra X-ray Observatory* and new developments in optical observations, we can revisit this relation, exploring the correlation of physically motivated quantities: the amount of hot gas and the independently determined gravitational potential depth of ETGs. As shown in Section 3, we have found a tight correlation between $L_{X,Gas}$ and M_{Total} with a small rms deviation of a factor of 3 in our 14 galaxy sample, which spans the entire range of measurable $L_{X,Gas}$; the rms deviation is even smaller, a factor of 1.3 for the 7 gas-rich galaxies ($L_{X,Gas} > 10^{40}$ erg s^{-1}). Mathews et al. (2006) reached a qualitatively similar conclusion, but they have instead used X-ray determined total mass among group-centered elliptical galaxies with $L_{X,Gas} = 10^{41}$–10^{44} erg s^{-1}, resulting in a larger scatter.

Since the gas temperature reflects the energy input and the depth of the potential well, the $L_{X,Gas}$–T_{Gas} relation provides a complementary scaling relation to $L_{X,Gas}$–M_{Total}. Interestingly, the functional form of this relation, which we have found in Section 3 (power law with $\alpha = 2.7 \pm 0.3$ or $\alpha = 3.3 \pm 0.3$ for gas-rich ETGs only) is consistent to what would be expected from the steep $L_{X,Gas}$–T_{Gas} relation found in BKF ($L_{X,Gas} \sim {T_{Gas}}^{4.5\pm0.6}$, where typically $kT = 0.3$–1 keV; see Figures 7 and 8 in BKF), for a gas in equilibrium. Given that $M_{Total} \sim {T_{Gas}}^{3/2}$ (virial theorem), we expect $L_{X,Gas} \sim {M_{Total}}^3$.

Our results indicate that the *total* mass of an ETG is the primary factor in regulating the amount of hot gas retained by the galaxy in the range of $L_{X,Gas} = 10^{38}$–10^{43} erg s^{-1} or M_{Total} = a few $\times$ 10^{10}–a few $\times$ 10^{12} $M_\odot$. By contrast, we note that the central binding energy (represented by the central stellar velocity dispersion σ) is less important, as shown by the large scatter in the $L_{X,Gas}$–σ relation (see Figure 5 in BKF). As suggested by recent observations, radio-mode AGN feedback appears to provide enough energy to prevent cooling of the hot ISM (e.g., Nulsen et al. 2007; Diehl & Statler 2008; also Fabian 2012). The tight $L_{X,Gas}$–M_{Total} relation implies that, at the present epoch, non-gravitational energy input is less important than the total mass in determining the gas retention capability of ETGs. The energy feedback may scale with the halo mass, if the DM halo determines the super-massive black-hole mass, as suggested by, e.g., Booth & Schaye (2010) as a possible variation of the popular relation between the black-hole and bulge masses (however, see also Kormendy & Bender 2011, who pointed out that M_{BH} is not correlated directly with the DM halo particularly for bulgeless galaxies). Even if it scales with the DM halo mass, feedback, although necessary to prevent cooling, cannot be more important than the halo mass in determining the gas retention capability.

The $L_{X,Gas}$–M_{Total} relation has more scatter for gas-poor galaxies with $L_{X,Gas}$ < a few $\times$ 10^{39} erg s^{-1} (Figure 1). A similar trend (i.e., larger scatter for galaxies with lower L_X) is also seen in the $L_{X,Gas}$–T_{Gas} plot (Figure 7 in BKF). These hot-gas-poor galaxies, where the gas is expected to be in the outflow state (e.g., Ciotti et al. 1991), may have a relatively small amount of DM, and consequently be unable to gravitationally confine the hot gas. In this case, various other factors may become significant, which are minor in gas-rich ETGs where DM dominates. Environmental effects could affect the amount of hot gas as a mechanism to remove hot gas by ram pressure stripping (as already seen in M84), or as a tool to better retain hot gas by adding the external pressure from the hotter ambient intracluster medium (see also Mulchaey & Jeltema 2010). However, even removing environmental effects and considering only isolated galaxies, the scatter may persist (see Memola et al. 2009). The dynamical properties and intrinsic

shape of ETGs may also become important. On average, at any fixed optical luminosity, rounder systems show larger L_X than flatter galaxies (e.g., Eskridge et al. 1995b). However, flatter systems also possess, on average, higher rotation levels (Sarzi et al. 2013) so that the binding energy is effectively lower (see Ciotti & Pellegrini 1996; Pellegrini et al. 1997). Other possibly important effects include the presence of cold ISM (e.g., Li et al. 2011) and rejuvenation (or stellar age), which could increase the stellar feedback (e.g., Sansom et al. 2006).

The $L_{X,Gas}$–L_K relation (Figure 2) is very steep ($L_{X,Gas} \sim L_K{}^{4.5\pm0.8}$). To better understand this steep relation, we can consider another scaling relation between the total halo mass and the stellar mass. Numerical simulations suggest that the halo mass and the stellar mass (e.g., from SDSS) are related in the mass range of our interest ($L_K > 10^{10.5}\,L_\odot$), following a relation of the form $M_{Total} \sim M_\star{}^{1.7-2.5}$ at $z = 0$ (e.g., Moster et al. 2013). We find a similar relation between M_{Total} and L_K among our 14 ETGs. If we adopt this relation and assume $M_\star \sim L_K$, given the observed $L_{X,Gas} \sim M_{Total}{}^3$ relation, we obtain an extremely steep $L_{X,Gas} \sim L_K{}^{5-7.5}$ relation, which is steeper than, but still consistent with, the observed relation ($L_{X,Gas}$–$L_K{}^{4.5\pm0.8}$). We note that even if the $L_{X,Gas}$–L_K relation is consistent with the other tighter scaling relations, the large scatter in this relation makes it less useful as a predictive tool. For example, one should not use this relation to predict $L_{X,Gas}$ from L_K. Mulchaey & Jeltema (2010) reported a similarly steep relation $L_{X,Gas} \sim L_K{}^{3.9\pm0.4}$ among field ETGs, where the environmental effect (ram pressure stripping, infall, etc.) is minimal. It is important to confirm their results after properly subtracting the ABs and CVs emission.

For galaxies not dominated by an AGN, and ignoring the small AB+CV contribution (~10% of $L_{X,LMXB}$), the total X-ray luminosity of an ETG can be written as

$$(L_{X,Total}/10^{40}\ \mathrm{erg\ s^{-1}}) = (M_{Total}/3.2\times10^{11}\,M_\odot)^3 + (L_K/10^{11}\,L_{K\odot}).$$

Since the stellar-mass-to-light ratio, $M_\star/L_K$, is close to 1 in solar units (Bell et al. 2003) and $M_{Total}/M_\star \sim 2$ for $L_K \sim 10^{11}\,L_{K\odot}$ (Deason et al. 2012), the contributions from the hot gas and LMXBs are approximately comparable at $L_K \sim 10^{11}\,L_{K\odot}$ or $M_{Total} \sim$ a few $\times\,10^{11}\,M_\odot$. Above this critical $L_X \sim 10^{40}$ erg s^{-1}, the hot gas will dominate the total X-ray emission and below it the LMXBs will dominate. This critical L_X is approximately where the hot gas states change between inflows and outflows. It will be very useful to observationally determine the exact location of the division between inflows and outflows in terms of M_{Total} or $L_{X,Gas}$ to place strong constraints on theoretical model parameters. The currently available sample, however, lacks galaxies with an intermediate mass and hot gas luminosity, in the critical range ($L_{X,Gas} \sim 10^{40}$ erg s^{-1} or $M_{Total} \sim 5\times10^{11}\,M_\odot$).

5. SUMMARY AND CONCLUSIONS

In summary, our scaling relations can be written in a simplified form

$(L_{X,Gas}/10^{40}\ \mathrm{erg\ s^{-1}}) = (M_{Total}/3.2\times10^{11}\,M_\odot)^3$ from this work,

$L_{X,Gas} \sim T_{Gas}{}^{4.5}$ from BKF,

$L_{X,Gas} \sim L_K{}^{4.5\pm0.8}$ (with a large scatter).

By comparison, the scaling relations for clusters of galaxies, where the gas is hotter at $kT = 2$–10 keV, are $L_X \sim M^2$ and $L_X \sim T^3$ (e.g., Pratt et al. 2009) with a tendency that the L_X–T relation steepens for lower T (<3 keV) groups (e.g., Eckmiller et al. 2011). It is well known that these relations in clusters are significantly steeper than self-similar expectations, predicting $L_X \sim M^{4/3}$ and $L_X \sim T^2$ (e.g., Eke et al. 1998; Arnaud & Evrard 1999). Our relations in ETGs are even steeper than those of clusters. The cause of the steeper relations will be addressed in a forthcoming paper (D.-W. Kim et al., in preparation).

If the presence of a well defined $L_{X,Gas}$–M_{Total} relation with little scatter is confirmed in a larger sample of galaxies, this scaling relation will provide the basis for a new reliable way for measuring the total mass (and in particular DM content) of ETGs.

We thank Alis Deason, Silvia Pellegrini, Aaron Romanowsky, and Mark Sarzi for helpful discussions. The data analysis was supported by the CXC CIAO software and CALDB. We have used the NASA NED and ADS facilities, and have extracted archival data from the *Chandra* archives. This work was supported by NASA contract NAS8-03060 (CXC).

REFERENCES

Arnaud, M., & Evrard, A. E. 1999, MNRAS, 305, 631
Bell, E. F., McIntosh, D. H., Katz, N., & Weinberg, M. D. 2003, ApJS, 149, 289
Bender, R., Surma, P., Dobereiner, S., Mollenhoff, C., & Madejsky, R. 1989, A&A, 217, 35
Binney, J. 2004, MNRAS, 347, 1093
Booth, C. M., & Schaye, J. 2010, MNRAS Lett., 405, L1
Boroson, B, Kim, D.-W., & Fabbiano, G. 2011, ApJ, 729, 12 (BKF)
Canizares, C. R., Fabbiano, G., & Trinchieri, G. 1987, ApJ, 312, 503
Cappellari, M., Scott, N., Alatalo, K., et al. 2013, MNRAS, 432, 1709
Ciotti, L., D'Ercole, A., Pellegrini, S., & Renzini, A. 1991, ApJ, 376, 380
Ciotti, L., & Pellegrini, S. 1996, MNRAS, 279, 240
David, L. P., Jones, C., & Forman, W. 1991, ApJ, 369, 121
Deason, A. J., Belokurov, V., Evans, N. W., & McCarthy, I. G. 2012, ApJ, 748, 2
Diehl, S., & Statler, T. 2008, ApJ, 680, 897
Eckmiller, H. J., Hudson, D. S., & Reiprich, T. H. 2011, A&A, 535, 105
Eke, V. R., Navarro, J. F., & Frenk, C. S. 1998, ApJ, 503, 569
Ellis, S. C., & O'Sullivan, E. 2006, MNRAS, 367, 627
Eskridge, P., Fabbiano, G., & Kim, D.-W. 1995a, ApJS, 97, 141
Eskridge, P., Fabbiano, G., & Kim, D.-W. 1995b, ApJ, 442, 523
Fabbiano, G. 1989, ARA&A, 27, 87
Fabbiano, G. 2006, ARA&A, 44, 323
Fabian, A. C. 2012, ARA&A, 50, 455
Forman, W., Jones, C., & Tucker, W. 1985, ApJ, 293, 102
Harris, D. E., & Krawczynski, H. 2006, ARA&A, 44, 463
Kim, D.-W., & Fabbiano, G. 2010, ApJ, 721, 1523
Kormendy, J., & Bender, R. 2011, Nature, 469, 377
Kormendy, J., Fisher, D. B., Cornell, M. E., & Bender, R. 2009, ApJS, 182, 216
Kraft, R. P., Vázquez, S. E., Forman, W. R., et al. 2003, ApJ, 592, 129
Li, J.-T., Wang, Q. D., Li, Z., & Chen, Y. 2011, ApJ, 737, 41
Mathews, W., & Brighenti, F. 2003, ARA&A, 41, 191
Mathews, W., Brighenti, F., Faltenbacher, A., et al. 2006, ApJL, 652, L17
Memola, E., Trinchieri, G., Wolter, A., Focardi, P., & Kelm, B. 2009, A&A, 497, 359
Moster, B. P., Naab, T., & White, S. D. M. 2013, MNRAS, 428, 3121
Mulchaey, J. S., & Jeltema, T. E. 2010, ApJL, 715, L1
Nipoti, C., & Binney, J. 2007, MNRAS, 382, 1481
Nulsen, P., Jones, C., Forman, W. R., et al. 2007, in ESO Astrophys. Symp., Heating and Cooling in Galaxies and Clusters of Galaxies, ed. H. Böhringer, G. W. Pratt, A. Finoguenov, & P. Schueker (Berlin: Springer), 210
O'Sullivan, E., Forbes, D. A., & Ponman, T. J. 2001, MNRAS, 328, 461
Pellegrini, S. 2005, MNRAS, 364, 169
Pellegrini, S. 2010, ApJ, 717, 640

Pellegrini, S., Held, E. V., & Ciotti, L. 1997, MNRAS, 288, 1
Pratt, G. W., Croston, J. H., Arnaud, M., & Böhringer, H. 2009, A&A, 498, 361
Randall, S., Nulsen, P., Forman, W. R., et al. 2008, ApJ, 688, 208
Sansom, A. E., O'Sullivan, E., Forbes, D. A., Proctor, R. N., & Davis, D. S. 2006, MNRAS, 370, 1541
Sarazin, C. L. 1988, X-ray Emissions from Clusters of Galaxies (Cambridge: Cambridge Univ. Press)
Sarzi, M, Alatalo, K., Blitz, L., et al. 2013, MNRAS, 432, 1845
Tonry, J. L., Dressler, A., Blakeslee, J. P., et al. 2001, ApJ, 546, 681
Trinchieri, G., & Fabbiano, G. 1985, ApJ, 269, 447
White, R. E., III, & Sarazin, C. L. 1991, ApJ, 367, 476